Available online at www.sciencedirect.com
ScienceDirect
Journal of Hazardous Materials 150 (2008) 290–299
Journal of Hazardous Materials
www.elsevier.com/locate/jhazmat

Safe disposal of toxic chrome buffing dust generated from leather industries

S. Swarnalatha [a], T. Srinivasulu [b], M. Srimurali [b], G. Sekaran [a,*]

[a] *Department of Environmental Technology, Central Leather Research Institute, Adyar, Chennai 600 020, Tamil Nadu, India*
[b] *Department of Civil Engineering, Sri Venkateswara University, Tirupathi 517502, Andra Pradesh, India*

Received 17 November 2006; received in revised form 18 April 2007; accepted 19 April 2007
Available online 24 April 2007

Abstract

The high concentration of trivalent chromium along with organic/inorganic compounds in chrome buffing dust (CBD), the solid waste discharged from leather industries, causes severe groundwater contamination on land co-disposal and chronic air pollution during thermal incineration. In the present investigation, CBD was subjected to starved air incineration (SAI) at 800 °C in a thermal incinerator under different flow rates of oxygen to optimize the oxygen required to incinerate the organic compounds and simultaneously preventing the conversion of Cr^{3+} to Cr^{6+}. The energy audit of SAI of buffing dust under the external supply of oxygen was carried out under different incineration conditions. The bottom ash from SAI was effectively solidified/stabilized using Portland cement and fine aggregate. The solidified blocks were tested for unconfined compressive strength and heavy metal leaching. Unconfined compressive strength of the blocks was in the range of 120–180 kg/cm^2. The stabilization of chromium(III) in the cement gel matrix was confirmed using Scanning Electron Microscopy SEM, Electron Paramagnetic Resonance spectroscopy (EPR) and X-ray diffraction spectroscopy (XRD). Leachability studies through TCLP on solidified blocks were carried out to determine the degree of leaching of chromium and organic compounds (expressed as COD) under standard conditions.

Keywords: Chrome buffing dust; Starved air incineration; Chromium; solidification/stabilization; Portland cement

1. Introduction

The tanning industry generates a huge quantum of liquid and solid wastes while producing finished leather. Tanning is the main process followed in leather manufacturing that protects the leather against some environmental effects such as microbial degradation, heat, sweat or moisture, etc [1]. In tanning industry raw skins/hides are transformed into leather by means of a series of chemical and mechanical operations [2,3]. The tanning process is usually accomplished in three distinct phases, i.e., preparation of the raw live stock to tan with tanning agents, tanning with mineral/vegetable tanning agents and post tanning to impart colour to finished leather. Basic chromium sulfate is the most widely used tanning agent for converting putrescible collagen fibres into non-putrescible leather matrix. Chrome tanned leathers have improved mechanical resistance, extraordinary dyeing suitability and better hydrothermal resistance in comparison with vegetable tanned leather. The solid wastes generated from leather industry can be broadly classified into untanned collagenous, tanned collagenous and non-proteinaceous wastes. Among the tanned collagenous waste, the one resulting from the finishing operation is called chrome buffing dust (CBD). CBD is a micro fined solid particulate impregnated with chromium, synthetic fat, oil, tanning agents and dye chemicals. About 2–6 kg of CBD is generated as a solid waste per ton of skin/hide processed. CBD contains chromium, it is carcinogenic in nature and it causes clinical problems like respiratory tract ailments, ulcers, perforated nasal septum, kidney malfunction [4] and lung cancer [5] in humans exposed to the environment containing buffing dust particulates. Hence, it is advised by pollution control authorities to collect the CBD for safe disposal.

The current methods for disposing buffing dust are land co-disposal and thermal incineration. Land co-disposal method is not preferred for the reasons such as overall high pollution emissions and low energy recovery. The thermal treatment method is preferred for its reduction in volume of solid waste to be

* Corresponding author. Tel: +91 44 24410232; fax: +91 44 24410232.
E-mail address: ganesansekaran@hotmail.com (G. Sekaran).

0304-3894/$ – see front matter © 2007 Elsevier B.V. All rights reserved.
doi:10.1016/j.jhazmat.2007.04.100

disposed off. The thermal treatment of solid wastes involves incineration, gasification and pyrolysis as the means of disposal, with the emphasis to recover energy from the waste. The investment cost for gasification is higher than thermal incineration and land co-disposal methods. But, cost of the thermal incineration process is only about 1/6th of the total cost for the landfilling scenario [6]. And also the available landfill sites rapidly reach their total capacity and the authorization for new sites becomes difficult [7]. So, the thermal incineration is considered as the cheapest alternative and attractive method for its simultaneous energy production and volume reduction of solid waste. The thermal incineration of tannery solid waste, particularly CBD, needs a special attention on the issues such as release of toxic chromium(VI), halogenated organic compounds, polyaromatic hydrocarbons etc. into the environment [8].

The major species formed from Cr (III) during thermal incineration of solid wastes are $Cr_2(SO_4)_{3(s)}$, $CrOCl_{2(g)}$ and $Cr_2O_{3(s)}$ which later accounts a path for the formation of Cr (VI) [9,10]. Solid waste composition and oxygen concentration in the incinerator determine the extent of conversion of Cr^{3+} to Cr^{6+}. Attempts have been made to inhibit the formation of these species under the limited oxygen supply conditions. In the present investigation, the CBD generated from a garment leather manufacturing industry was subjected to starved air incineration (SAI) to utilize its maximum calorific value as well as to inhibit the oxidation of Cr^{3+} to Cr^{6+}. The process produced bottom-ash containing toxic heavy metals mainly Cr^{3+} and partially burnt carbon. The highly toxic properties of bottom ash prohibit its direct land co-disposal. Therefore, an effective solidification/stabilization of bottom ash was resorted to change potentially hazardous solid wastes into less hazardous or non-hazardous solids before it is disposed off as landfill [11,12]. SAI initially suffered operational problems due to the release of volatile organic compounds and partially converted carbon oxides in the flue gas. This was controlled by catalytic combustion of flue gas over nickel impregnated ceramic granules of diameter 7 mm (0.05 g of Ni/g of ceramic granule) at 450 °C using air as an oxidant. The flue gas from catalytic converter was scrubbed in a scrubber to remove acidic vapors using alkaline water.

Solidification is a process, which has been considered as an alternative solution to the wastes containing heavy metals. Solidification and stabilization (s/s) processes are applicable to a wide variety of industrial wastes as a treatment step prior to long–term storage on land. The objectives of s/s are: (i) to immobilize the contaminants through chemical and physical mechanisms in order to reduce the rate at which the contaminants can be transported to the environment and (ii) to increase the structural integrity of the treated material. Wastes containing heavy metals are often treated with alkaline and cementing agents to precipitate the metal ions in free form and to yield a solid matrix of desirable strength. During solidification with Portland cement, hydration reaction produces a calcium-silicate-hydrate (C-S-H) gel representing a meta stable precursor of crystalline phases such as tobermorite and jennite. These phases and the formation of ettringite are responsible for creating filamentous structures that coat and hold the heavy metal particles together [13,14].

In the present study the bottom ash was solidified/stabilized using Portland cement, fine aggregate, coarse aggregate and blue metal dust. The focal theme of the present investigation was on:

(i) to arrest oxidation of trivalent chromium to hexavalent chromium with simultaneous energy utilization from organic fractions
(ii) solidification and stabilization (s/s) of bottom ash of CBD;
(iii) leachability studies on solidified/stabilized bricks to determine the metal fixation

2. Material and methods

2.1. Chrome buffing dust (CBD) and its characteristics

Chrome buffing dust used in the study was collected from a garment leather manufacture industry in Chennai, Tamil Nadu. CBD was dried for two weeks and utilized in further experiments.

The dried CBD was characterized for moisture content, ash content, chemical oxygen demand (COD) and total organic carbon (TOC) according to the APHA standard methods [15]. Chromium(III) (Cr^{3+}) and chromium(VI) (Cr^{6+}) was characterized according to the DIN protocol. Thermo-gravimetric analysis such as (TGA), elemental analysis carbon, hydrogen, nitrogen and sulphur (CHNS), SEM, electron paramagnetic resonance (EPR), Fourier transform infrared (FTIR) and calorific value studies were carried out to determine the thermal stability of waste, elemental composition, morphology, oxidation state of chromium in the waste, functional groups and recoverable energy in the CBD respectively.

2.1.1. Estimation of chromium(III) and chromium(VI)

About two grams of the CBD samples was gently stirred for 3 h with 100 ml of 0.13 moles of dipotassiun hydrogen ortho phosphate at pH 8 and filtered. Out of it, 10 ml of the solution was added with 10 ml of phosphate buffer and made upto 25 ml. One ml of 0.5% diphenyl carbazide was added followed by the addition of 0.5 ml of ortho phosphoric acid. The solution was kept for colour development for 15 min and the absorbance was measured at 540 nm. The calculated concentration was chromium(VI).

Total chromium was estimated using the above method after digesting the samples using acid mixtures (5 ml HNO_3: 3.5 ml H_2SO_4: 11.5 ml $HClO_4$) followed by the oxidation using potassium permanganate and sodium azide. Chromium(VI) is subtracted from total chromium to get chromium(III).

2.1.2. TGA

TGA was carried out to determine the weight loss with respect to temperature in order to fix the heating segment pattern of incineration. The dried samples were analyzed under nitrogen atmosphere using Seiko Instruments (Japan). The samples were heated in a platinum pan from 40 to 800 °C at the rate of 20 °C/min. The mass of CBD used in TGA was 2.5 mg.

2.1.3. Calorific value

Gross calorific value (GCV) was measured using DIN 51900. A Parr adiabatic bomb with a Parr Calorimeter Controller 1720 was used. The heat of combustion of CBD was determined by measuring the temperature increase in the calomel water and then calculated from energy balance of the system.

2.1.4. Elemental (CHNS) analysis

The elemental CHNS content of the uncalcined CBD was determined using CHNS 1108 model Carlo–Erba analyzers. The ratio of oxygen to mass of CBD was calculated using the modified Dulong formula [16].

2.2. Starved air incineration of chrome buffing dust

The schematic flow diagram of Starved air incineration and solidification/stabilization of calcined CBD are shown in Fig. 1. The dried CBD was charged in a stainless steel (316 grade) vertical retort of weight 13 kg, which was placed in an electrical furnace. The CBD was incinerated at 800 °C with a provision to supply gas mixture (N_2: O_2 90: 10 w/w) to collect and to treat the off gases discharged from the furnace. SAI was operated with a gradual increase in temperature to 800 °C in six segments for about 8 h as shown below:

- Segment I: Ambient temperature → 100 °C (rate of heating at 100 °C h^{-1})
- Segment II: 100 °C → 300 °C (rate of heating at 100 °C h^{-1})
- Segment III: 300 °C → 400 °C (rate of heating at 50 °C h^{-1})
- Segment IV: 400 °C → 600 °C (rate of heating at 200 °C h^{-1})
- Segment V 600 °C → 800 °C (rate of heating at 200 °C h^{-1})
- Segment VI: 800 °C → 800 °C (soaking for 1 h)

The flushing of the gas mixture was stopped in the segment V and VI to avoid the conversion of trivalent chromium(Cr^{3+}) to hexavalent chromium(Cr^{6+}). The outer jacket of the lid of the incineration vessel was covered with glass wool of 6 mm thickness in order to prevent condensation of volatile organic compounds back into incinerator, which increases energy recovery efficiency and prevents the heat dissipation from the reactor. The incinerator was designed to operate the process under controlled reaction temperatures and reaction time using a microprocessor. The energy consumption was recorded by means of an energy meter (India Meters Ltd., India). The record of energy consumption and recovery for constant weight of the dried CBD (400 g) was carried out in the present investigation at different airflow of 1.5, 2.25, and 3.0 g/min of oxygen. The bottom ash generated during the incineration process was collected in a tray provided at the bottom of the furnace. The flue gas from the incinerator was scrubbed in a scrubber. The scrubber is a PVC column of height 1.5 and 0.175 m diameter to remove acidic vapors using alkaline water. Water required for scrubbing the flue gas was provided through a pump of capacity 0.5 HP. Provisions were made for characterizing the scrubbing solution used in the scrubber. The flue gas free from acidic vapors was further oxidized at 450 °C over Ni-coated ceramic granules (0.05 g

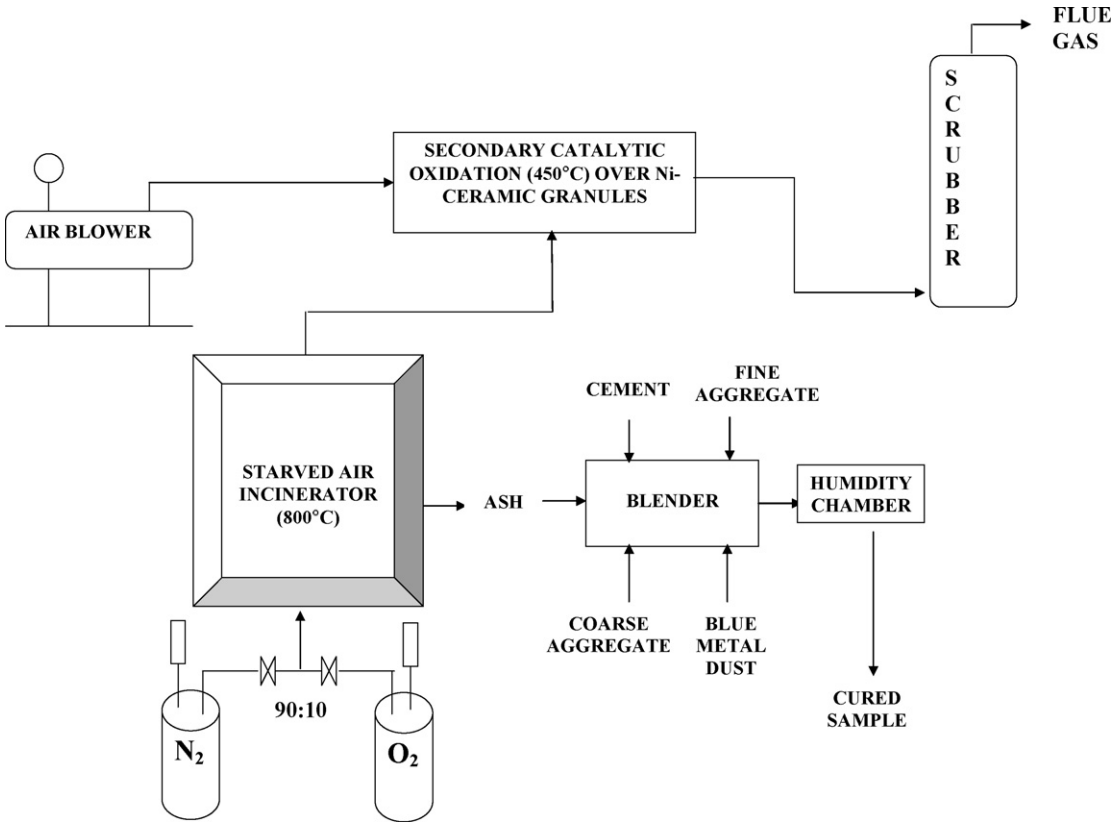

Fig. 1. Starved air incineration and solidification/stabilization system for chrome buffing dust discharged from a garment leather manufacturing industry.

of Ni/g) under the flux of air (30 l/min) in a separate reactor to oxidize the unconverted hydrocarbon and carbon monoxide to stable end products. The bottom ash collected from the incinerator was subjected to characterization such as EPR, SEM, FT–IR studies and elemental analysis (CHNS).

2.3. Solidification and stabilization

2.3.1. Preparation of concrete blocks

The bottom ash was collected from the furnace after calcination of CBD was powdered and quantified. Cold molding technique was applied to prepare the solidified concrete blocks. Concrete blocks, measuring 7.5 cm × 5 cm × 10 cm, were made using polymethacrylate sheet of thickness 3 mm for cold molding. Portland cement 43grade (RAMCO Cements, TamilNadu) was used as a binder for solidification of bottom ash because of their cheapness and availability. Besides, Portland cement and calcined CBD coarse aggregate, fine aggregate and blue metal dust (obtained from a stone crushing unit) in different proportions (Table 1) were used for making solidified blocks. It was made into wet plastic mass using water and homogenized in an extruder and casted into moulds. The casted blocks were removed from the moulds after two days and cured for 28 days in a constant humidity chamber, made of polyacrylic material. Unconfined compressive strength (UCS) of the cured concrete blocks was determined in accordance with the procedure of ASTM D2850.

2.3.2. Instrumental analysis of uncalcined CBD, calcined CBD and solidified blocks

2.3.2.1. FTIR studies. Investigation on the functional groups present in the samples was carried out using FTIR (Perkin Elmer spectrophotometer). The FTIR analysis was carried out for uncalcined CBD, calcined CBD and control block. The powdered samples were mixed with KBr of spectroscopic grade and pressed into disk of dimensions 10 mm in diameter and 1 mm in thickness. The samples were scanned in the spectral range of 400–4000 cm^{-1}.

2.3.2.2. EPR studies. EPR spectra were recorded on a Bruker (Ettlingen, Germany) EPR 300X–band EPR spectrometer at room temperature. Five milligrams of the dried and powdered uncalcined, calcined CBD block samples were placed in a quartz sample tube of diameter 5 mm and then subjected to EPR analysis. An X-band microwave with a power of 1 mW and frequency of 9.771 GHz was applied to the specimen.

2.3.2.3. Surface morphology of the concrete block (SEM). Surface morphology of uncalcined CBD, calcined CBD, and calcined CBD – fine aggregate – cement block was examined using Leica Stereo Sean 440 scanning electron microscope (SEM). The sample was coated with gold by a gold sputtering device for a clear visibility of the surface morphology.

2.3.2.4. XRD studies. The structural compositional study of the block was carried out using Philips X'pert diffractometer for 2θ values ranging from diffraction angles from 10 to 80° using Cu Kα radiation at $\lambda = 1.54$ Å. The other experimental conditions included 1/2° divergence slits and 5 s counting time at each step and intensity measured in counts. The '*d*' value was calculated using the Bragg's diffraction equation $2d \sin\theta = n\lambda$.

2.4. Leachability test

The leachability of the metals from the solidified samples of calcined CBD blocks were determined by Toxicity Characterization of Leachate Procedure test (TCLP). TCLP is designed to determine the mobility of both organic and inorganic analytes present in liquid, solid and multiphasic wastes. It is usually used to determine EP toxicity of a hazardous waste.

The cured samples were crushed, powdered and homogenized (greater the surface area, more is the leachability) [17,18] to pass through 600 μm screens. The powdered sample of weight 20 g was placed in a TCLP cylinder with 400 ml of extraction fluid (5.7 ml of glacial HOAc in 500 ml of water and then adjust to pH 4.95). The contents were agitated in a TCLP rotatory agitator at 30 rpm for 18 h and the liquid phase was separated from the solid phase by filtration through a 0.6–0.8 μm borosilicate glass fiber under pressure of 50 psi (340 KPa). The liquid phase was analyzed for pH, COD, TOC and trivalent chromium ion to determine metal fixation efficiency.

3. Results and discussion

3.1. Characteristics of buffing dust

The moisture content, ash content, COD, TOC, Cr^{3+} and Cr^{6+} of the CBD were 37.4%, 43.4%, 760 mg/g, 290 mg/g, 8.9 mg/g, <100 μg/ml (BDL) respectively. Gross calorific value of the CBD was 3838 Kcal/kg.

3.1.1. TGA

TGA of uncalcined CBD (Fig. 2) shows that the weight loss at 98.3 °C is due to elimination of moisture. The organic compounds of CBD such as tannin, synthetic tannin, protein and fatty substances are hydrophilic in nature and thus the water molecules are held in the bound form. TGA records a weight loss in the temperature ranges from 280.6 to 589 °C, which

Table 1
Unconfined compressive strength of the stabilized–solidified blocks

Sample No.	Percentage composition of the solidified/stabilized blocks	Unconfined compressive strength (kg/cm^2)
CB1	C – Fa (50.0–50.0)	146.67
SB1	CBD – C – Fa (33.33–33.33–33.33)	120.00
CB 2	C-Fa- Ca (33.33–33.33–33.33)	173.34
SB 2	CBD-C-Fa-Ca (33.33–33.33–16.66–16.66)	80.00
CB 3	C-Fa-Bd (33.33–33.33–33.33)	146.67
SB 3.	CBD-C-Fa- Bd (33.33–33.33–16.66–16.66)	80.00

CB, control block; SB, sample (calcined buffing dust) block; CBD, calcined buffing dust; C, cement; Fa, fine aggregate; Ca, coarse aggregate; Bd, blue metal dust.

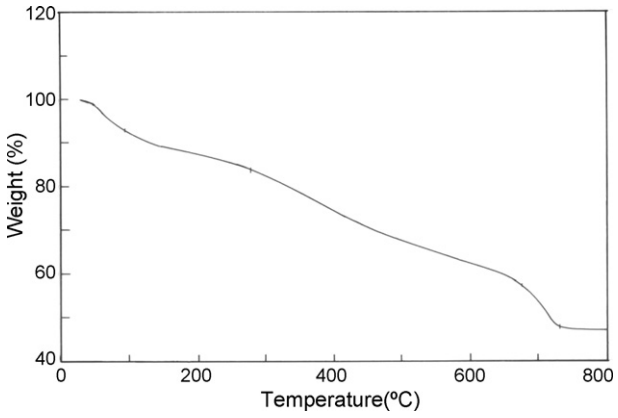

Fig. 2. TGA spectrum of uncalcined chrome buffing dust.

can be attributed to the decomposition of organic compounds in the uncalcined buffing dust into intermediate compounds. The intermediate compounds were volatilized off that left behind the ash content in the temperature range from 630.2 to 732.1 °C.

3.1.2. Elemental analysis

The elemental composition of the buffing dust was Carbon 42.8%, Hydrogen 8.099%, Nitrogen 8.113%, Sulphur 1.846% and Oxygen 30.98%. The elemental analysis suggests that the CBD contains inorganic components as 8.162% including 0.885% of chromium.

3.2. Starved air incineration of tannery chrome buffing dust

The dried CBD was incinerated under starved air at 800 °C at different O_2 flow rate 1.5, 2.25 and 3.0 g/min. The main aim of the present investigation is to prevent the oxidation of Cr^{3+} to Cr^{6+} while maintaining the incineration of organic compounds in CBD. The following advantages are expected in SAI:

- Heat recovery from CBD.
- The resulted residue will meet the requirement for solidification and stabilization using Portland cement.
- Bottom ash can be replaced for sand in concrete.
- Disposal volume of CBD will be reduced.

The SAI was carried out at constant loading rate of 400 g of CBD and the following terminologies are used in deriving energy balance of the CBD incineration:

- Heat energy liberated in SAI = q_T
- Heat energy lost in heating stainless steel retort = q_1
- Heat energy consumed in heating gas (O_2: N_2) mixture entering into the reactor = q_2
- Heat energy lost in glass wool in the Outer jacket of the lid of the vertical reactor = q_3
- Total Heat lost during starved air combustion, $q_N = q_1 + q_2 + q_3$
- Net heat energy change (Δq) in SAI = $q_T - q_N$

q_1, q_2, q_3 were calculated using m$C\Delta$T, where 'm' was the mass of the materials, ΔT the temperature rise and 'C' is the specific heat capacity of the materials.

The relationship between net energy change (Δq) and furnace temperature is shown in Fig. 3. It is evident from the energy profile graph that the incineration of CBD occurs in three stages, which correlates with the TGA of the CBD.

- Stage I:
  Net heat energy change (Δq) is positive in this stage, which means that heat energy was absorbed by the system. This results in energy loss due to the surface and bound water movement and also towards the emission of volatile organic compounds from CBD.
- Stage II:
  Net heat energy change (Δq) is negative, which means that heat energy was released from CBD. This is associated with the combustion of the organic fraction of the CBD.
- Stage III:

Net heat energy change (Δq) is positive; heat energy was absorbed by the system possibly for the decomposition of inor-

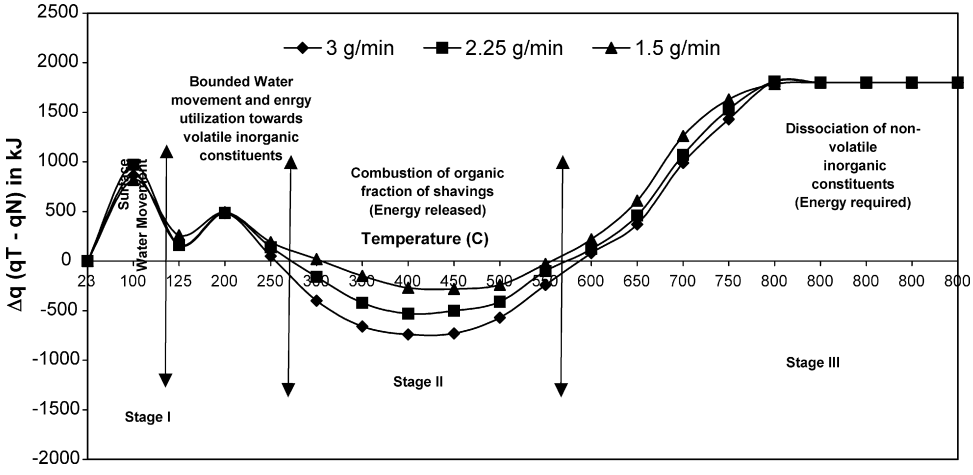

Fig. 3. Effect of oxygen flow rate for net energy change (Δq) with respect to furnace temperature in correlation with TGA.

Table 2
Total energy consumed (q_T) for incineration of chrome buffing dust in the temperature range of 23 °C (ambient temperature) to 800 °C at various oxygen flow rate

Rise in temp. (°C)	Total energy in kJ (q_T) at different oxygen flow rate		
	1.5(g/min)	2.25(g/min)	3(g/min)
23–100	1400	1440	1440
100–125	455.9	360	360
125–200	1080	1080	1080
200–250	615.8	562.7	440.
250–300	445.8	262.7	−10
300–350	274.1	−4.4	−215.5
350–400	154.1	−114.4	−295.5
400–450	94.1	−126.6	−352.1
450–500	134.1	−36.6	−192.1
500–550	344	273.4	137.9
550–600	594	493.4	457.9
600–650	984	807	717
650–700	1634	1417	1337
700–750	2004	1877	1777
750–800	2160	2160	2160
800.0–800.0	1800	1800	1800
800.0–800.0	1800	1800	1800
800.0–800.0	1800	1800	1800
800.0–800.0	1800	1800	1800
$\sum q_T$	19573.9	17651.2	16041.6
$\sum q_N$	6057.4	5819.02	5938.3
$\Delta q \sum q_T - \sum q_N$	33.8	29.58	25.3

$\sum q_T$ = Sum of q_T. $\sum q_N$ = Sum of q_N; $q_N = q_1 + q_2 + q_3$.

ganic compounds in CBD, to maintain temperature of the reactor at 800 °C and for the heat retained in the bottom ash.

The total heat energy of the system (q_T) in each stage of SAI of CBD for the varied loading of CBD is presented in Table 2. Although the algebraic sum of Δq for varied loading of CBD at different furnace temperatures are positive (absorption of the energy by the system), the magnitude of Δq was decreased for increased airflow, i.e., +25.3 kJ/g for oxygen flow of 3 g/min while it is +33.8 kJ/g for airflow of 1.5 g/min.

Bottom ash yield after the incineration was 70.5 g for O_2 flow of 3 g/min, 83.5 g for O_2 flow of 2.3 g/min and 101.5 g for O_2 flow of 1.5 g/min of oxygen. Gross calorific value (GCV) of CBD was 15.9 kJ/g, therefore it is expected that from the incinerated material the total energy recovery should be 5,228.8 kJ for O_2 flow of 3 g/min, 5,023.5 kJ for O_2 flow of 2.25 g/min and 4,737.5 kJ for O_2 flow of 1.5 g/min but the experimental observation was contrary to the theoretical prediction. Energy was drawn from the external energy source rather than to be recovered. The possible energy losses in the process are illustrated below:

(i) the energy recovered in the temperature range of 280.6–589 °C (region of thermal decomposition of organic fraction as evidenced from TGA) is 9.9 kJ/g (3260 kJ for 329.5 g of combustible CBD), 6.7 kJ/g (2000 kJ for 316.6 g of combustible CBD) and 2.4 kJ/g (730 kJ for 298.5 g of combustible CBD) for O_2 flow of 3, 2.25 and 1.5 g/min respectively. The values suggest that, at oxygen flux rate 3.0 g/min the energy released in the temperature range of 280.6–589 °C satisfied the theoretical demand to some extent while at low oxygen flux rates the observed and expected energy values are much deviated. This is attributed to the insufficient supply of oxygen.

(ii) the stoichiometric oxygen requirement for complete combustion of C, H, N and S of CBD to CO_2, H_2O, NO_2 and SO_2 respectively is 797.12 g. The oxygen supplied at temperature range 280.6–589 °C for the oxygen flux rate of 1.5, 2.25 and 3.0 g/min respectively were 33.9, 50.8 and 67.7% of the stoichiometric oxygen requirement. The starved air was supplied for the purpose of arresting the conversion of trivalent chromium to hexavalent chromium because the toxic hexavalent chromium species like CrO_2Cl_2 tends to form at incinerating temperature 425 °C and CrO_3 begins to form at 527 °C and more Cr (VI) species form in the presence of excess oxygen supply at higher temperatures [10]. Therefore, oxygen supply rate of 3 g/min addresses both better energy recovery as well as complete arrest of oxidation of trivalent chromium to hexavalent chromium. Even though, energy is recovered in the temperature range 280.6–589 °C for the oxygen rate of 3 g/min., the overall energy consumption was (as recorded by the energy meter) 10,103.3 kJ.

(iii) flue gas retains some amount of energy as evidenced from the measured temperature of the flue gases (Table 3). The loss of heat due to the energy carried by the flue gases such as CO_2, SO_2, NO_2 and water vapour (calculated using C, H, N and S content of CBD) is 222.3, 4.27, 41.28 and 752.84 kJ respectively.

(iv) the loss of heat in the SAI was also due to absorption of heat energy by the system possibly for maintaining the reactor at 800 °C and for the decomposition of inorganic compounds apart from the heat retained in the bottom ash.

The large amount of heat was utilized in the segment V and VI, which can be attributed to the energy retained in the bottom ash [19]. More energy was supplied in this section for the purpose of lowering the mass of the calcined CBD and also to make the calcined CBD more compatible with cement–gravel mixture used in solidification/stabilization process by reducing the carbon percentage to a greater extent. Thus, SAI can be made effective if the following conditions are met:

Table 3
Temperature of furnace compared with the temperature of flue gas

Furnace temp. (°C)	Flue gas temperature at furnace outlet (°C) and at different oxygen flow rate		
	1.5 (g/min)	2.25 (g/min)	3.0 (g/min)
100	28	28	29
200	60	78	80
300	189	200	205
350	251	250	255
400	287	300	313
500	343	363	372
600	450	463	467
700	540	547	591
800	613	616	622

- Reduction of moisture content of CBD before loading the incinerator
- Good house keeping of CBD before loading in SAI
- Minimization of energy loss (q_N) through sound engineering design of incinerator

The chromium(III) present in the calcined CBD was estimated as 50.2 mg/g.

3.3. Instrumental interpretations

3.3.1. FTIR studies

FTIR analysis of the dried uncalcined and calcined CBD was carried out in the frequency range between 400 and 4000 cm^{-1}. The FTIR spectrum of uncalcined CBD is shown in Fig. 4a. There is a broad envelope in the higher energy region 2800 and 3700 cm^{-1}. The peak centered at 3399.78 cm^{-1} can be assigned to overlapping of –OH stretch of water and –NH stretch of protein group. The intense bands lying around 1655.45 and 1561.29 are attributed to the C=O stretching vibration and N–H bending vibration of protein molecules respectively. The intense peaks at about 875.57 and 712 cm^{-1} are attributed to the Cr (III) species [20].

Fig. 4b illustrates the FTIR spectrum of the calcined sample. There is only a medium O-H stretching band centered at 3424.35 cm^{-1} corresponding to the bound water molecules in the CBD. During incineration of CBD, proteins are converted into amino acids and then into smaller fragments such as NH_3 and carbon dioxide group. The absence of 1655.30 and 1553.91 cm^{-1} confirms the above. Absence of alteration in the bands near 875.57 and 712 cm^{-1} confirms the prevention of Cr (III) to Cr (VI) conversion in starved air incinerator.

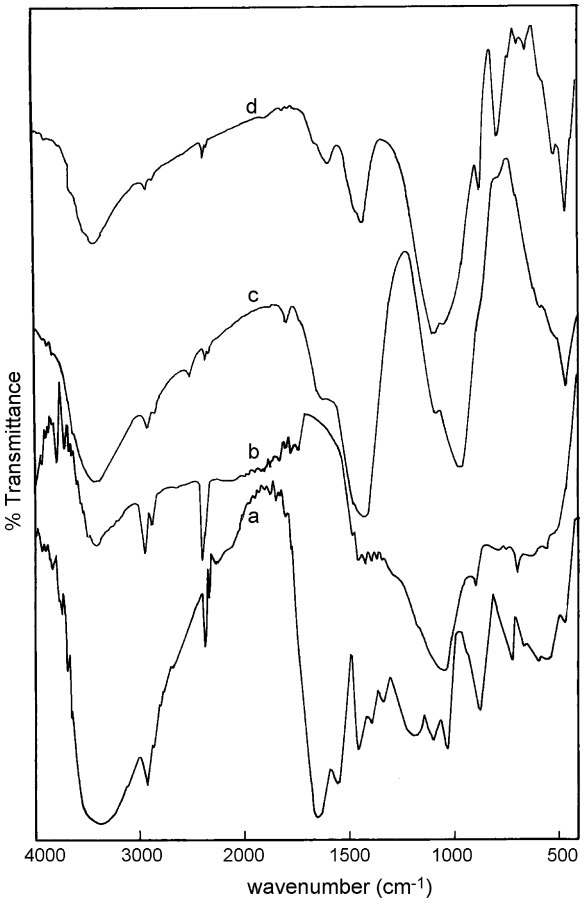

Fig. 4. FTIR spectra of (a) uncalcined buffing dust, (b) calcined buffing dust, (c) control block and (d) bottom ash block.

The FTIR spectra of the solidified control block and bottom ash concrete block are shown in the Fig. 4c and d. A broad envelope from 3700–2900 cm^{-1} can be assigned to –OH stretch of calcium hydroxide. The Si–O–Si anti symmetric stretching in hydrated cement is seen typically around 970 cm^{-1}. The band due to Si–O–Si symmetric stretching in the C–S–H at 943 cm^{-1} is not clearly seen which could be due to the polymerized form of the structure. A small shoulder at 1089.4 cm^{-1} can be attributed to the quartz resulted from fly ash. A strong band around 1425 cm^{-1} was assigned to calcite present in the matrix. In Fig. 7b, there is a great shift in Si–O–Si anti symmetric stretching, which confirms the immobilization of calcined CBD in cement – coarse aggregate matrix. The presence of peaks at 875.57 and 783.41 cm^{-1} apart from the control block clearly confirm that the Cr^{+3} is effectively stabilized in the ettringite.

3.3.2. EPR studies

EPR spectra of uncalcined and calcined buffing dust are shown in Fig. 5a and b. A positive EPR signal for trivalent chromium (containing unpaired electron) and a negative EPR signal for Cr (VI) (with no unpaired electron) is expected. The electronic levels for Cr^{3+} ion with its three unpaired electrons gives a total spin $S = 3/2$ in an octahedral crystal field [21]. Thus, the presence of Cr^{3+} is exhibited by a symmetrical band centered at about $g = 2.04$ [20].

The EPR spectrum of calcined CBD suggests that there is no alteration in the symmetrical bands, which confirms that the conversion of Cr^{3+} to Cr^{6+} was avoided in SAI. This was also confirmed by quantitative analysis of the bottom ash. It is evident from the spectrum that the bottom ash contained free electrons; this is correlated with the g-factor at 2.0068. Besides the evidence for chromium, the spectrum also showed the evidence for strong free electron at the g-factor of 2.0068. The pyrolysis of proteinaceous compounds into amorphous carbon through free radical mechanism can be the reason for the presence of free electrons in the bottom ash.

The EPR spectrum of solidified block centred at g-factor of 2.04 (Fig. 5c) clearly reveals the presence of chromium. This clearly indicates that the calcined CBD was effectively embedded in the cement – coarse aggregate matrix. Thus, the solidification of the calcined CBD in concrete matrix proves to be an effective stabilization method.

3.3.3. SEM analysis of uncalcined and calcined CBD

Fig. 6a and b illustrate the scanning electron micrograph of uncalcined and calcined CBD. The morphology reveals the dense packed layer in the uncalcined CBD and interspaces in the dense packed layer of calcined CBD

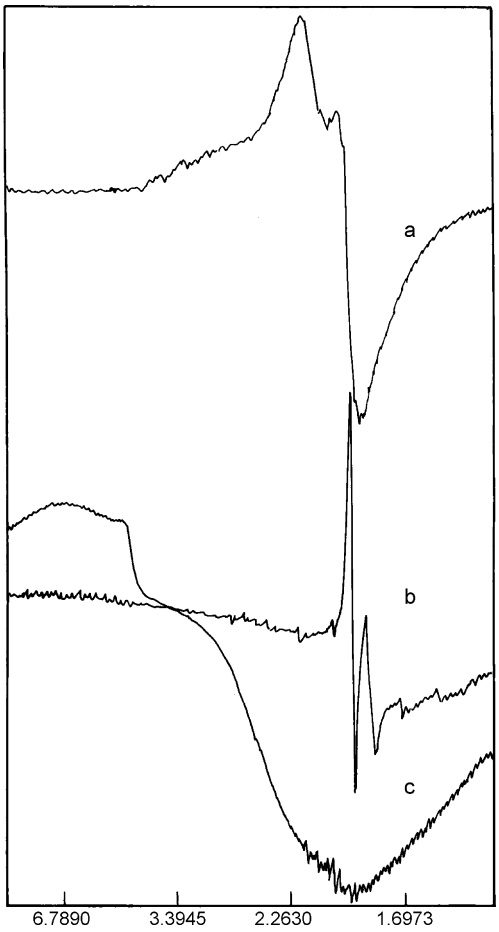

Fig. 5. EPR spectra of (a) uncalcined buffing dust, (b) bottom ash and (c) solidified blocks.

The SEM of solidified block is shown in the Fig. 7.

Hydration of $Ca_3Al_2O_6$ in the presence of cement yields ettringite phase having the molecular formula $3CaO.\ Al_2O_3 \cdot 3CaSO_4 \cdot nH_2O$ as shown below

$$1Ca_3Al_2O_6 + 3(CaSO_4.1/2H_2O) + 26H_2O \leftrightarrow Ca_6(Al(OH)_3)_2(SO_4)_3 \cdot 26H_2O(\text{cement})$$

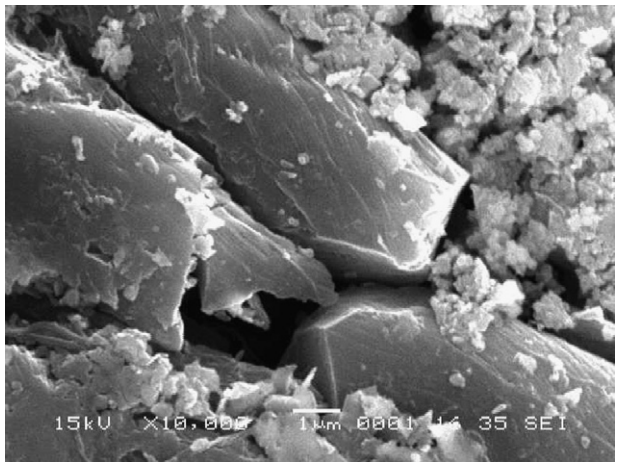

Fig. 7. SEM images of the ettringite structure present in the calcined CBD embedded in concrete matrix.

The ettringite phase formed favors isomorphous substitution of Al^{3+} by Cr^{3+} in the calcined CBD.

3.4. Solidification/stabilization

3.4.1. Unconfined compressive strength (UCS) of calcined CBD blocks

The concrete blocks of the mentioned compositions were prepared and tested for UCS (Table 1). UCS of the mixtures varied with the proportions of the additives.

The compositions of the control blocks were chosen as per the different usage in the construction industry. The composition of cement – fine aggregate (CB1) is used for the low cost hollow cement blocks. And the composition of cement – fine aggregate – coarse aggregate (CB2) is generally used for rich mix concrete purpose whereas cement – fine aggregate – blue metal dust (CB3) is used for the wearing coat of the pavement. The sample blocks designated by SB1, SB2 and SB3 were the calcined CBD mixed with the concerned composition. Comparision of CB1 and SB1 reveal that the compressive strength was decreased by about 25.27 kg/cm^2, which can be attributed to the low percentage of cement in SB1 than in CB1. There exists a great difference in the compressive strength among the pairs

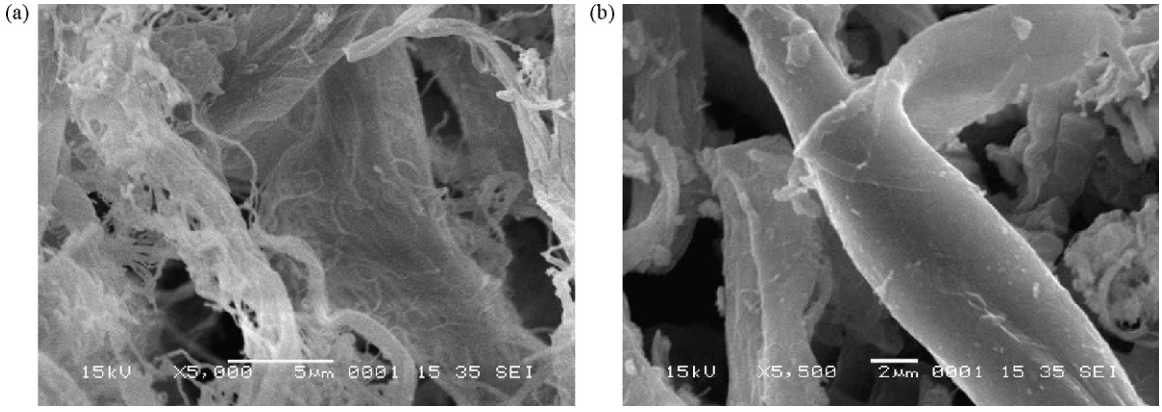

Fig. 6. Surface morphology of (a) uncalcined buffing dust, (b) calcined buffing dust.

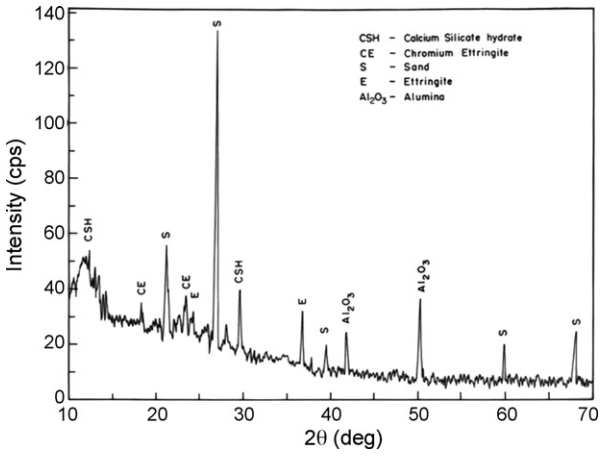

Fig. 8. XRD spectrum of the bottom ash embedded in concrete matrix.

of CB2 and SB2, CB3 and SB3. The difference in compressive strength is due to percentage differences of fine aggregate, coarse aggregate and blue metal dust. So, the addition of calcined CBD to the low cost hollow cement bricks will be the most appropriate method for the utilization of the bottom ash of SAI.

3.4.2. XRD analysis

XRD analysis of the solidified block (Fig. 8) indicates the pozzolanic product formation. Calcium silicate hydrate (CSH) and Al_2O_3 were the main products identified apart from the presence of sand peaks. Chromium immobilized in ettringite phase as $3CaO.Cr_2O_3{\cdot}3CaSO_4.nH_2O$ is indicated by the 2θ angles at 18.35° and 22.32° apart from the ettringite phase at 24.13 and 36.67°.

3.5. Leachability studies

Leachabiltiy tests are used to assess:

a) Hazardous nature of the waste
b) Effectiveness of the solid waste treatment process
c) Suitability of solidified and stabilized solid wastes for land co-disposal.

The concentrations of COD, TOC and Cr^{3+} in the leachate after 18th hour TCLP test for the concrete specimen having the highest compressive strength are 64, 31 and 0.51 mg/l. The TCLP study suggested that the leachate contained Cr^{6+} at BDL (below detectable limit) and chromium fixation percentage as calculated by Swarnalatha et al. [20] is 99.99%.

An interesting observation of this study was that Cr^{3+} and COD concentration in the leachate were less than that demanded by the standards (5 and 280 mg/l for Cr^{3+} and COD respectively) [22] which proved the success of solidifying the incinerated tannery waste under starved air.

4. Conclusions

The study deals with the starved air incineration of CBD generated from leather industry under varied rates of oxygen supply (3, 2.25 and 1.5 g/min) at 800 °C and detailed investigation was carried out for effective utilization of combustion energy without the conversion of trivalent chromium to hexavalent chromium. Though net energy change indicates that energy was drawn from the external sources rather than to be recovered, the detailed investigation shows that the energy of the organic fractions were incinerated to the maximum extent at the O_2 flow rate of 3.0 g/min. The conversion of trivalent chromium to the hexavalent in the process was absolutely prohibited, which was confirmed through the instrumentation techniques such as EPR and FTIR. The bottom ash of CBD was solidified and investigated for the best mode of disposal as low cost hollow cement bricks. The leaching characteristics through TCLP confirmed the effective stabilization of chromium i.e. the metal fixing capacity was 99.99%. The effective stabilization of chromium(III) in the blocks was evidenced by 875.57 and 712 cm^{-1} peaks in FTIR, g-factor at 2.04 in EPR, ettringite phase shown in SEM and 2θ angle at 24.13 and 36.67° in XRD analysis.

The study concludes that the organic fractions of CBD can be destructed with out oxidizing trivalent chromium into hexavalent chromium through starved air incineration at 800 °C and there is a scope for better recovery of energy from buffing dust. The resultant bottom ash can be solidified and stabilized using cement and fine aggregate. The solidified block can be used as low cost hollow cement blocks for its compressive strength and metal fixation capacity.

Acknowledgments

The authors are thankful to the Director, central leather research institute (CLRI) for providing the facility to carry out the work and the author S. Swarnalatha is thankful to council of scientific and industrial research (CSIR) for awarding the senior research fellowship.

References

[1] G. Sekaran, K. Shanmugasundaram, M. Mariappan, Characterization and utilization of buffing dust generated by the leather industry, J. Hazard. Mater. B63 (1998) 53–68.
[2] A. Cassano, E. Drioli, R. Molinari, Recovery and reuse of the chemicals in unhairing, degreasing and chromium tanning processes by membranes, Desalination 113 (1997) 251–261.
[3] A. Cassano, E. Drioli, R. Molinari, Saving of water and chemicals in tanning industry by membrane process, Water Res. 4 (1999) 443–450.
[4] A.H.G. Love, chromium – biological and analytical considerations, in: D. Burrows (Ed.), Chromium metabolism and toxicity, CRC Press, Boca Raton, FL, 1983, p. 1.
[5] A. Leonard, R.R. Lawverys, Carcinigenicity and mutagenicity of chromium, Mutat. Res. 76 (1980) 227–239.
[6] G. Assefa, O. Eriksson, B. Frostell, Technology assessment of thermal treatment technologies using ORWARE, Energy Convers. Manage. 46 (2005) 797–819.
[7] D.W. Kirk, C.C.Y. Chan, H. Marsh, Chromium behaviour during thermal treatment of MSW fly ash, J. Hazard. Mater. B90 (2002) 39–49.
[8] European Commission, Directorate – General JRC, Joint Research Centre, Institute for prospective technological studies (Seville), technologies for sustainable development, European IPPC Bureau, integrated pollution prevention and control (IPPC), reference document on best available techniques for the tanning of hides and skins, final draft/March 2001, http://eippcb.jrc.es.

[9] S. Skrypski-Mantele, T.R. Bridle, Environmentally sound disposal of tannery sludge, Water Res. 29 (4) (1995) 1033–1039.
[10] J. Chen, M.Y. Wey, B. Chiang, S. Hsieh, The simulation of hexavalent chromium formation under various incineration conditions, Chemosphere 36 (7) (2003) 1553–1564.
[11] A. Filibelix, N. Buyukkamaci, H. Senol, Solidification of tannery wastes, Resource Conserv. Recy. 29 (2000) 251–261.
[12] T.A. Ioaninides, J. Zouboulis, Detoxification of a highly toxic lead-loaded industrial solid waste by stabilization using apatites, J. Hazard. Mater. B97 (2003) 173–191.
[13] D.A. Kulik, M. Kersten, Aqueous solubility diagrams for cementitious waste stabilization systems: II, End-member stoichiometries of ideal calcium silicate hydrate solid solutions, J. Am. Ceram. Soc. 84 (12) (2001) 3017–3026.
[14] L.J.J. Catalan, E. Merliere, C. Chezick, Study of the physical and chemical mechanisms influencing the long-term environmental stability of natrojarosite waste treated by solidification/stabilization, J. Hazard. Mater. B94 (2002) 63–88.
[15] S.C. Lenore, E.G. Arnold, R.T. Rhodes, Standard methods for the examination of water and wastewater, vol. 1193, 17th ed., American Public Health Association, Washington, 1985.
[16] H.S. Peavy, D.R. Rowe, G. Tchobanogloas, Environmental Engineering, Mc Graw Hill International Editions, New york, 1985, pp. 584–585.
[17] J.R. Conner, Chemical fixation and solidification of hazardous wastes, Van Nostrand Reinhad Publisher, New York, 1990, pp. 26–30.
[18] B.I. Silveire, A.E.M. Dantas, J.E.M. Blasques, R.K.P. Santos, Effectiveness of cement based systems for stabilization and solidification of spent liquor inorganic fraction, J. Hazard. Mater. B98 (2003) 183–190.
[19] S. Swarnalatha, K. Ramani, A. Geetha Karthi, G. Sekaran, Starved air combustion – solidification/stabilization of primary chemical sludge from a tannery, J. Hazard. Mater. B137 (2006) 304–313.
[20] S. Swarnalatha, M. Arasakumari, A. Gnanamani, G. Sekaran, Solidification/stabilization of thermally – treated toxic tannery sludge, J. Chem. Technol. Biotechnol. 81 (2006) 1307–1315.
[21] A. Nakajima, Y. Baba, Mechanism of hexavalent chromium adsorption by persimmon tannin gel, Water Res. 38 (2004) 2859–2864.
[22] C.J. Sollars, R. Perry, Cement-Based stabilization of wastes: Practical and theoretical considerations, J. Inst. Water Environ. Manage. 3 (2) (1989) 125–132.